Preprints of the 21st IFAC World Congress (Virtual)
Berlin, Germany, July 12-17, 2020

Optimization of the electric efficiency of the electric steel making process

Jesús D. Hernández *, Luca Onofri****
Sebastian Engell*

** Process Dynamics and Operations Group, Department of Biochemical and Chemical Engineering, Technische Universitat Dortmund, Emil Figge-Str. 70, 44221 Dortmund, Germany (e-mail: Sebastian.engell@ tu-dortmund.de).*
*** Acciai Speciali Terni (AST), Vle. Benedetto Brin 218, 05100 Terni, Italy.*

Abstract: This paper reports numerical and practical results of an open-loop optimal control formulation that reduces the power consumption of the electric arc furnace (EAF) steel production process. A control vector parametrization technique is used to optimize the batch trajectory with the goal to minimize the energy losses of the process. First principles models are utilized to describe the dynamics, as well as the influence of the voltage and impedance set-points on the process. The results of the dynamic optimization provided a sequence of set-points (called a melting profile) that aligns well with intuition: the profile utilizes high power levels during the high efficiency stages of the process, and low power levels as the batch moves towards a more energy inefficient state. The benefits of the proposed optimized mode of operation are demonstrated by an experimental study case. An optimal melting profile was calculated and implemented in a fully operative ultra-high power EAF. For a series of 19 test batches, the energy consumption and the batch time of the process were reduced by 4.5% and 4.6% for one type of steel.

Keywords: Dynamic optimization, advanced process control, process control applications, steel production, electric arc furnace, efficiency enhancement.

1. INTRODUCTION

The steel production process via electric arc furnaces (EAFs) is an energy-intensive process that during the last two decades has gained the attention of scientists and practitioners working in the areas of Advanced Process Control (APC). Early works utilized linearized models to implement Model Predictive Control (MPC) strategies aiming at improving the process conditions of the EAF (Bekker et al., 2000) (Coetzee et al., 2005) and their economics (Oosthuize et al., 2004) (MacRosty et al., 2007). More recently, complex nonlinear models have been employed in open-loop control, and integrated RTO-MPC strategies were proposed to optimize the economic performance of the process also considering the prices of electric power (Rashid et al., 2016).

Interestingly, the energy efficiency of the EAF process has not yet been addressed in the APC literature. In a nutshell, the main difference between the results obtained from either an energy efficiency driven or an economic driven optimization is that the set-points obtained by the latter can move the process to a very energy inefficient state if there is profit in doing so. This scenario is likely to occur, for example, if the electricity cost drops considerably during the final stages of a batch of steel – the period which is the most energy inefficient process phase (Hernandez et al., 2019a).

In this paper, we investigate and quantify the benefits of operating the process using an optimal melting profile which is obtained using dynamic optimization. To obtain an optimal mode of operation, an EAF process model and an electric arc model are embedded in a dynamic optimization problem that aims at minimizing the energy losses of the process. The outline of this paper is as follows: In section 2, we briefly describe the EAF process model and formulate the optimal control problem. The complexity of the problem is reduced by considering operational practices and by analysing the physical phenomena that govern the heat exchange during the batch. In section 3, we describe the computational algorithms used to simulate the EAF model and to solve the dynamic optimization problem. Section 4 presents the numerical results of the optimization and discusses the benefits of its implementation in a fully operative EAF. We conclude this paper with closing remarks in Section 5.

2. MATHEMATICAL MODELS

2.1. EAF process model

The main challenge in the application of APC strategies to the electric steel making process is that existing models lack the ability of describing the dynamic evolution of the most important states of the process (the masses and the temperatures of the liquid and solid phases) accurately. For example, existing state of the art EAF models (MacRosty et al. 2004) (Logar et al., 2012) (Meier et al., 2018) assume that the solid scrap has a cone frustrum geometry during the melting stage of a batch. This assumption is questionable not only

because it does not align well with our observations of the process in the ultra-high power EAFs at Acciai Speciali Terni (AST), but also because the melting rates that it predicts are higher than the ones observed at the plant. A major shortcoming about this assumed geometry is that the walls of the furnace remain covered during most of the batch. Therefore, the radiation losses through these surfaces are underestimated.

In earlier works (Hernandez et al., 2019a-b), we developed an EAF process model that considers the EAF as a system of three phases: solid metal, liquid metal, and the gaseous atmosphere. Furthermore, our model assumes that the solid scrap has a hollowed cylinder geometry as the metal melts, see Fig. 1.

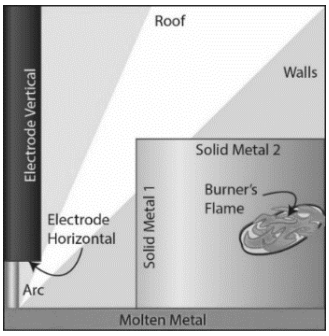

Fig. 1 Radial cut of the furnace geometry

In comparison to previous models (Bekker et al., 1999) (Logar et al., 2012) (Meier et al., 2018), our model predicts more accurately the melting rates, the batch times, and the energy consumption of the process. The improved performance of our model results from the use of (a) the hollowed-cylinder geometry; (b) a stricter treatment of the radiative heat exchange (shadings and blockages in exchanges are considered), and (c) the consideration of physical mechanisms that describe more accurately the heat released by the oxidation reactions in the liquid and solid phases of the process. A detailed description of model is out of the scope of this paper and will be provided in future work. Due to lack of space we can only summarize its main features:

- The dynamics of the melting process are modelled using a simplified system of only four state variables: the mass and the temperature of the solid and liquid metal phases, which were derived from the mass and energy balances.

- The power exchanges among the various surfaces in the EAF enclosure (arc, molten metal, solid metal, electrode horizontal, electrode vertical, walls and roof) are estimated using the DC circuit analogy technique and the view factors are calculated using a Monte Carlo approach. (Hernandez et al., 2019a)

- The influence of the set-points of the oxyfuel burner on the efficiency of the furnace is considered by means of a first principles dynamic model of the oxy-fuel flame (Hernandez et al., 2019b), see Fig. 2.

- The model predicts the evolution of the masses and the temperatures of the solid and liquid phases in the system; the radiative energy fluxes to every surface in the EAF enclosure; the energy contributions due to the oxidation of metals in the liquid and solid phases, as well as those occurring due to the liquid metal splashing, and the combustion of the oxy-fuel flames and coal.

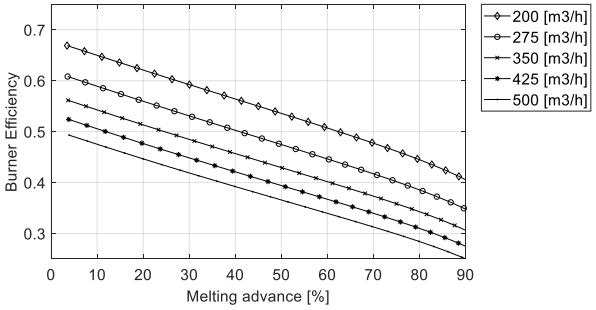

Fig. 2 Burner efficiency for various methane flow-rates

In this work, the power gains ($\dot{Q}_{gain}$) and the power losses ($\dot{Q}_{loss}$) of the process are defined as follows:

$$\dot{Q}_{gain} = \dot{Q}_{sm} + \dot{Q}_{mm} \quad (1)$$

$$\dot{Q}_{loss} = \dot{Q}_{roof} + \dot{Q}_{wall} + \dot{Q}_{elev} + \dot{Q}_{eleh} \quad (2)$$

In (1) and (2), $\dot{Q}_{sm}$, $\dot{Q}_{mm}$, $\dot{Q}_{wall}$, $\dot{Q}_{elev}$, $\dot{Q}_{eleh}$ represent the energy fluxes absorbed by the solid metal, molten metal, the wall, the roof, and the vertical and horizontal surfaces of the electrodes.

2.2. Optimal control problem

The electrical energy efficiency optimization of the EAF steel production process can be formulated as the problem to minimize the losses over the batch time, constrained to the physics of the melting process, the operational constraints of the electrical transformer, and the required final temperature of the melt (3).

$$\text{minimise} \quad \int_{t=0}^{tf} \dot{Q}_{loss}\big(V_a(t), Z_a(t), t_f\big).dt \quad (3)$$

subject to

- Dynamic model: evolution of the masses and temperatures of the metal phases

- Algebraic equations: heat exchanges between the energy sources and the metal phases

- Relationship between the electrical set-points and energy irradiated by the arc

- Constraints: maximum and minimum voltage and power of the furnace

- Terminal constraint: required final temperature of the melt.

The major difference between (3) and earlier formulations of the optimal control problem is that we solve the problem in terms of the voltage $V_a(t)$ and the impedance $Z_a(t)$ set-points of the electric arcs. This makes it possible to consider the influence of the electrical phenomena of the electric arc on the physics of the metal melting process.

Solving (4) poses a challenging dynamic optimization problem that can be simplified if (a) the physics of the electric arc are decoupled from the heat exchange problem (but not ignored) (b) if operative practices are also taken into account.

First, an important consequence that follows from the fact that steel making electric arcs are radiation dominated is that the heat exchanges can be estimated without knowing the temperature of the arc. This is because regardless of its voltage and impedance set-points, the arc will always emit the same amount of radiative energy at the same power level. Second, it is possible to demonstrate that regardless of the power level and the stage of the melting process (excluding the refining stage), the longer the arc, the more energy is transmitted from the arc to the solid scrap (due to lack of space, this proof is not included here). These two factors lead to decouple the physics of the plasma column from that of the heat exchange between the arc and the other phases in the enclosure because, on the one hand, they imply that the electrical set-points of the EAF influence the melting process only by means of the power level that they set and by the length of the arc that results.

On the other hand, if operations follow the strategy of using a single impedance level throughout the batch, not only the number of variables in (3) is reduced to half the number of the original variables, but also a single impedance level implicitly determines both a unique voltage of operation and a unique arc length at every power level. This implies that during the optimization, it is not required to search for the set of voltage and impedance set-points that generate the longest arc. The length and the power of the electric arc are related to the arc voltage by equations (4) and (5):

$$l_a = \frac{V_a - 40}{11.5} \tag{4}$$

$$P_a = \frac{{V_a}^2}{Z_a} . \cos \emptyset. \tag{5}$$

Efficient heat transfer from the arc to its environment also depends on the stability of the arc. Unfortunately, the higher the impedance set-point, the more unstable the arc becomes. In practice, an electric arc is considered stable if a power factor ($\cos \emptyset$) larger than 0.78 is guaranteed. Therefore, in this work, the largest impedance value for which the power factor was larger than 0.78 in the whole operative voltage range of the furnace was chosen as the operative set-point. By choosing the largest impedance set-point, we implicitly achieve the longest possible arc at all voltage and power levels.

At the selected impedance level, equations (4) and (5) can be combined to obtain a correlation between the power and the length of the electric arc. Fig. 3 presents this relationship for impedance setpoints at 6, 7, 8 and 9 mΩ, considering $\cos \emptyset = 0.82$.

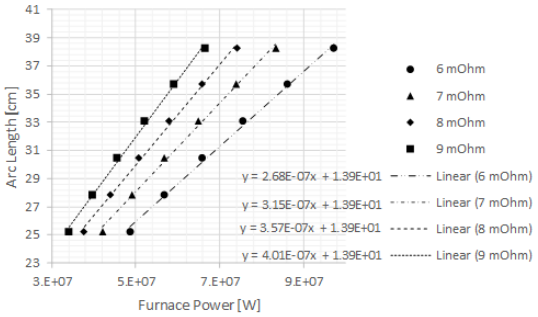

Fig. 3 Electric arc length vs. operative power level

The above considerations lead to a reformulation of (3) in terms of the arc power that still takes into account the correlations between the electrical set points of the arc, its geometry, and the heat exchange between the arc and the other surfaces in the EAF.

$$\begin{aligned} &\text{minimise} && \int_{t=0}^{tf} \dot{Q}_{loss}(P_a(t), t_f).\, dt \\ &&& \text{- Dynamic model} \\ &&& \text{- Algebraic equations} \\ &\text{subject to} && \text{- } l_a = f(P_a) \\ &&& \text{- Operative constraints} \\ &&& \text{- Terminal constraint} \end{aligned} \tag{6}$$

3. SOLUTION METHOD

The optimization problem in (6) was implemented and solved in MATLAB® using a sequential dynamic optimization approach (Biegler, 2010).

3.1. Numerical solution of the EAF process model

The structure of the EAF model makes it possible to solve the dynamic and algebraic systems independently without the need of a DAE solver. A two-time grid simulation structure was used to overcome the convergence issues that the integrator had with the statistical method of calculation of the view factors (Monte Carlo method) which is embedded in the model.

On the coarse grid, that consists of 1 minute intervals, the energy contributions from each source are computed independently by means of nonlinear solvers; logic if-else structures (within the Monte Carlo method of calculation of view factors), and linear matrix operations.

The dynamic system was solved with the standard `ode45` integrator, taking as inputs the already computed energy contributions from each energy source. Here, the time resolution was automatically set by the algorithm (this generates the fine grid of the simulation). The solution of the

dynamic system is done for each 1-minute interval of the coarse grid.

In this simulation approach, most of the computational load results from the Monte Carlo calculation of the view factors which takes approximately 200 ms. On average, the simulation of a batch of two charges took around 7 CPU seconds in a computer using an Intel® CoreTM i7-8750H processor with 16GB of RAM.

3.2. Numerical solution of the optimization problem

The optimization problem was solved parametrizing the input vector in 10 intervals of constant length. This discretization was chosen as it guarantees that the operative power level is not changed before the process runs for at least 10 times the settling time of the control system of the electrodes at any given power level.

The optimization was solved using an SQP solver and the gradients were estimated using finite differences. The solution aimed at finding the optimal profile of the electric power input for a batch of two charges.

The main benefit of this solution method is that an a priori knowledge of the batch time is not required because the integrator can be stopped at the point at which the terminal conditions are met (on the coarse grid). From an implementation point of view, this strategy requires the input vector to have at least 12 components, the expected 10 plus 2 spares, that allow the integrator to proceed for longer periods if the terminal constraints are not met.

4. RESULTS AND DISCUSSIONS

4.1. Numerical case study

4.1.1. Batch simulation

Even though operative practices vary widely from melt shop to melt shop, a general practise is to operate the furnace at a constant power level throughout the whole batch. When this is the case, the electrical energy optimization problem boils down to the problem of finding a set of voltages and impedance set-points that reduce the length of the electric arc as the batch progresses. The goal of this mode of operation is to reduce the radiative losses from the arc to the walls and to the roof of the EAF.

The effect of the electrical set-points on the radiative heat exchange during the batch is shown in Fig. 4. The voltage, impedance and arc length values used in the simulation are presented in a normalized manner in Table 1. Here, the normalization bases are the maximum operative voltage (V_a), the maximum arc length obtained for the selected voltage level (l_a), and the impedance required to obtain the operative power level. (Z_a)

Step	V_a	Z_a	l_a	Step	V_a	Z_a	l_a
1	1	1	1	6	0.94	0.88	0.93
2	0.94	0.88	0.93	7	0.88	0.77	0.86
3	0.88	0.77	0.86	8	0.81	0.66	0.80
4	0.81	0.66	0.80	9	0.75	0.56	0.76
5	1	1	1	10	0.75	0.56	0.76

Table 1. Voltage, impedance, and arc length over the simulation timeline at a normalized power level of 1 [MW/MW]

The energy fluxes arriving at each participating surface of the EAF system, for a batch of two charges, are presented in Fig. 4. Here, the mass of solid material loaded in the EAF during each charge is the same. The energy fluxes are presented in a normalized fashion with respect to the maximum power of the transformer. The arc length is normalized with respect to the maximum arc length, as in Table 1.

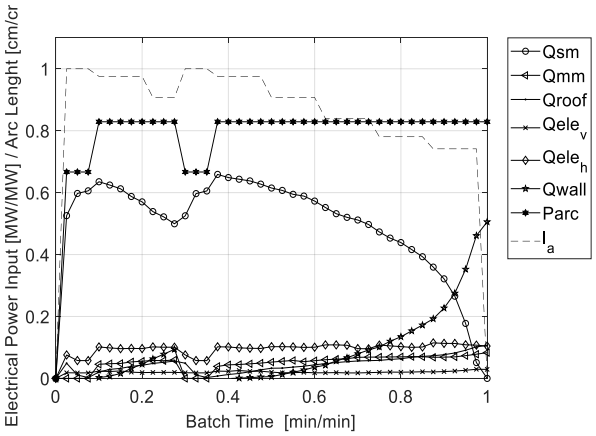

Fig. 4 Normalized energy fluxes vs. normalized batch time for the profile in Table 1

In Fig. 5, the energy flux to the metal and the energy losses during the batch, as defined in (1) and (2), are presented. Considering that the fluxes are normalized w.r.t. the power of the arc, Fig. 5 can also be understood as the dynamic efficiency curve of the process.

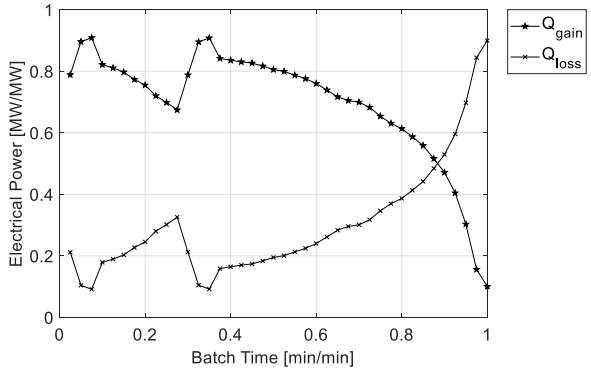

Fig. 5 Electrical efficiency and losses of the EAF process if operated according to the profile in Table 1

The results in Fig. 5 lead to three observations: First, the process is highly efficient immediately after each loading of the furnace: the solid metal absorbs as much as 83% of the energy irradiated by the arc. Second, the energy efficiency of the process decreases as the batch time progresses. Third, the process is particularly inefficient during the last 10% of the batch time because a large percentage of the energy irradiated by the arc is absorbed by the walls and the roof of the EAF.

Based on these observations, one can formulate the following hypothesis:

Hypothesis 1: The energy performance of the process could be improved if operations follow a control philosophy that introduces more energy when the process is more efficient, and less energy when the process is less efficient.

4.1.2. Batch Optimization

The dynamic optimization problem (6) was solved using a stair-shaped decreasing power input vector as initial guess. The average power of this vector was equal to the stationary power level of the simulated batch in the previous sub-section. Here, a normalized operative impedance value of 0.88, and a constant $\cos\emptyset = 0.82$ were assumed. The computed optimal profile, energy fluxes, and arc lengths over the batch run are presented in Fig. 6.

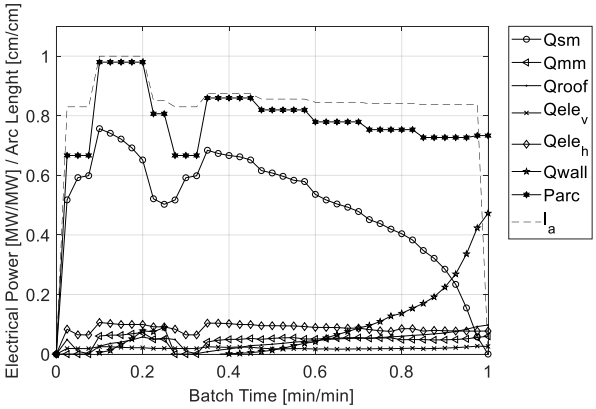

Fig. 6 Optimal melting profile for the numerical case study

In comparison to the base case, the optimal profile in Fig. 6 utilizes higher power levels at the beginning, and lower power inputs at the end of the batch. After the second charge, the power level is slightly increased from the level at which the first charge terminated, but it remains well below the maximum power level utilized during the first batch. An important difference between Fig. 5 and Fig. 6 is the length of the operational arc. While in the base case the length of the arc decreases considerably over time (around 22%), for the optimal case, the arc length remains almost constant throughout the second charge.

Fig. 7 shows a comparison between the reference case and the computed optimal profile in terms of three important KPIs: the batch time, the energy losses, and total energy demand. These results suggest that with the optimal power profile, the energy demand and the losses of the process can be reduced by almost 2% and 4%, respectively. On the other hand, batch time remains almost unchanged as it decreased by only 1%. Operations with lower energy losses are desirable not only because they lead to more energy efficient operations, but also because the wear of the refractory of the walls and the electrode consumption are reduced.

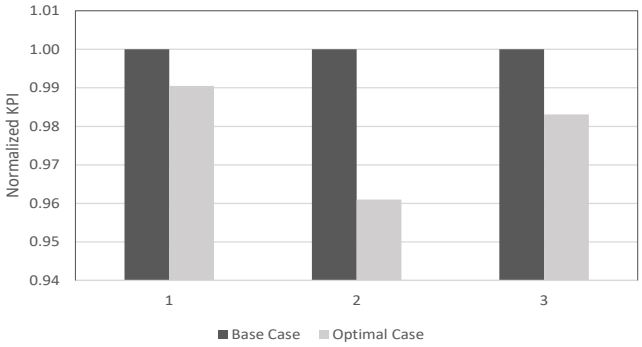

Fig. 7 Normalized KPIs for the base case, and the optimal profile. KPI 1: Batch Time. KPI 2: Total energy losses. KPI 3: Total energy demand

4.2. Experimental results for the real process

The optimization framework was employed to obtain optimal profiles for two different grades of stainless steel. In real operations, the loading practices (number of charges, mass charged in each load, etc.) and the physical properties of the metal scrap (density, heat capacity, latent heat of fusion), are different from those of the numerical simulations carried out in section 4.1. The detailed results of these computations cannot be disclosed to protect industrial know-how. The computed optimal profiles were implemented in one of the industrial Ultra High Power EAF (UHP-EAF) at AST and 19 tests batches were run. For these batches, the average energy demand and the batch times are compared with the average data of one year of production. The results of these calculations are presented in a normalized manner in Fig. 8 and Fig. 9.

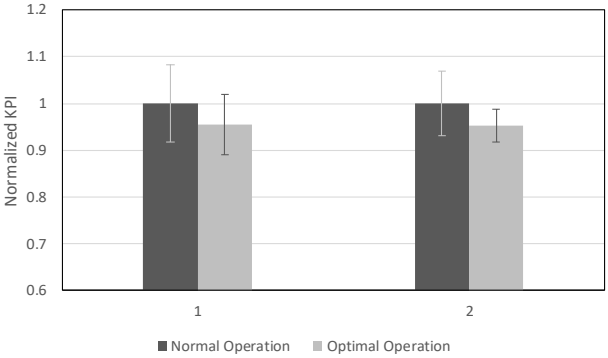

Fig. 8 Batch time and Energy demand improvements for steel grade A. KPI 1: Batch time. KPI 2: Energy demand.

On average, the optimal profile reduced the energy demand of steel A by 4.6% and that of steel B by 1.7%. In terms of the batch time, a reduction of 4.5% was achieved for steel grade

A, and no improvement was observed for steel grade B. The results of these experiments proved that the model-based optimization computes a mode of operation that performs better than the traditional operative practices, with different amounts of savings for different steel grades.

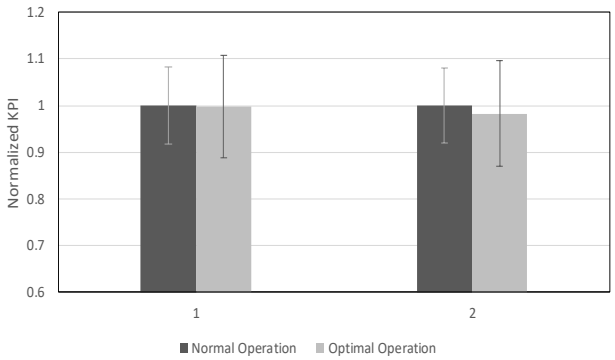

Fig. 9. Batch time and Energy demand for steel grade B. KPI 1: Batch time. KPI 2: Energy demand.

5. CONCLUSIONS

In this work, we presented and validated an optimization framework that improves the energy performance of the steel production process in electric arc furnaces (EAF). A control vector parametrization technique was used to solve the optimization problem to minimize the energy losses of the process. The algorithm computed a mode of operation that reduces the operational power over while maintaining constant the length of the arc throughout most of the batch.

One major advantage of the employed cost functional in the optimization is that it computes modes of operation that improve both the economics and the energy efficiency of the process. By reducing the energy losses, the algorithm handles in an implicit manner the two largest costs of the process: the electrical energy and the electrode consumption. We demonstrated the effectiveness of the optimization framework by computing and testing an optimal melting profile in an operative UHP-EAF for two different grades of steels. For these two cases, energy savings of 4.6% and 1.7% were achieved. We conjecture that the optimal point of operation for each batch is strongly influenced by the loading practices and the properties of the raw materials.

The numerical and experimental results give evidence that the energy performance of the EAF process can be improved by operating it at higher power levels during the periods where the process is highly efficient (immediately after each loading procedure), and progressively introducing less electric power as the batch progresses.

Operations at maximum electrical efficiency (minimum losses) lead to a trade-off between the batch time and the total energy consumption. In future work, we will explore evolutionary algorithms to tackle the multi-objective nature of this problem.

ACKNOWLEDGEMENTS

Financial support is gratefully acknowledged from the Marie Curie Horizon 2020 EID-ITN Project “PROcess NeTwork Optimization for efficient and sustainable operations of Europe’s process industries taking machinery condition and process performance into account - PRONTO”, Grant agreement No. 675215.

We would like to thank Mauro Grifoni and Lucio Mancini for valuable discussions about the EAF operations. We also acknowledge Daniele Sguigna and Roberto Moretti, for having supported and permitted the experimental trials on the EAF.

REFERENCES

Bekker, J. G., Craig, I. K. and Pistorius, P. C. (1999). Modeling and Simulation of an Electric Arc Furnace Process. *ISIJ International*, vol. 39, pp. 23-32, 1999.

Bekker, J. G., Craig, I. K. and Pistorius, P. C. (2000). Model predictive control of an electric arc furnace off-gas process. *Control Engineering Practice*, vol. 8, pp. 445-455.

Biegler L. T. (2010). *Nonlinear programing. Concepts, algorithms and application to chemical processes*. Society for Industrial and Applied Mathematics. Pittsburgh, PA, USA.

Coetzee, L. C., Craig, I. K., and Rathaba L. P. (2005). MPC control of the refining stage. *IFAC proceedings volumes,* vol. 38, Issue 1, pp. 151-156.

Hernandez, J. D., Onofri, L., and Engell, S. (2019a). Detailed modelling of radiative heat transfer in Electric Arc Furnaces using Monte Carlo Techniques. *Proc. of the 8th International SteelSim Conference*, *Toronto, Canada*, pp, 295-304. Association for Iron & Steel Technology.

Hernandez, J. D., Onofri, L., and Engell, S. (2019b). Model of an Electric Arc Furnace Oxy-Fuel Burner for dynamic simulations and optimization purposes. *IFAC PapersOnLine,* 52-14, pp. 30–35.

Logar V., Dovzan D. and Skrjanc I. (2012). Modeling and Validation of an Electric Arc Furnace: Part 1, Heat and Mass Transfer," *ISIJ International*, vol. 3, p. 402–412.

MacRosty, R. D., and Swartz, C. L. (2005). Dynamic Modeling of an Industrial Electric Arc Furnace. *Ind. Eng. Chem. Res.*, vol. 44, pp. 8067-8083.

MacRosty, R. D., and Swartz, C. L. (2007). Dynamic Optimization of Electric Arc Furnace Operation. *AIChE Journal*, vol. 53, no. 3, pp. 640-653.

Meier T., Gandt K., Hay T. and Echterhof T. (2018) Process Modeling and Simulation of the Radiation in the Electric Arc Furnace. *Steel Research International,* vol. 89, no. 4, p. 1700487.

Oosthuize, D. J., Craig, I. K., and Pistorius, P. C., (2004). Economic evaluation and design of an electric arc furnace controller based on economic objectives. *Control Engineering Practice*, vol. 12, pp. 253-265.

Rashid, M. M., Mhaskar, P., and Swartz, C. L. (2016). Multi-rate modeling and economic model predictive control of the electric arc furnace. *Journal of Process Control*, vol. 40, pp. 50-61.